Characterization of electroless nickel-phosphorus plating for ultracold-neutron storage

H. Akatsuka[g], T. Andalib[b], B. Bell[a], J. Berean-Dutcher[a], N. Bernier[a,d], C.P. Bidinosti[e,b], C. Cude-Woods[c], S.A. Currie[c], C.A. Davis[a], B. Franke[a,d], R. Gaur[a], P. Giampa[m], S. Hansen-Romu[b], M.T. Hassan[c], K. Hatanaka[f], T. Higuchi[f], C. Gibson[a], G. Ichikawa[h,j], I. Ide[g], S. Imajo[f], T.M. Ito[c], B. Jamieson[b,e], S. Kawasaki[h], M. Kitaguchi[g], W. Klassen[d], E. Korkmaz[l], F. Kuchler[n], M. Lang[b,e], M. Lavvaf[b], T. Lindner[a,e], M. Makela[c], J. Mammei[b], R. Mammei[a,e,b], J.W. Martin[e,b], R. Matsumiya[a,f], E. Miller[d], K. Mishima[h,j], T. Momose[d,a], S. Morawetz[a], C.L. Morris[c], H.J. Ong[f,p], C.M. O'Shaughnessy[c], M. Pereira-Wilson[a], R. Picker[a,i], F. Piermaier[a,k], E. Pierre[a,f], W. Schreyer[a,*], S. Sidhu[a,i], D. Stang[a,k], V. Tiepo[a], S. Vanbergen[d,a], R. Wang[d], D. Wong[c,o], N. Yamamoto[g]

[a] *TRIUMF, Vancouver, BC V6T 2A3, Canada*
[b] *University of Manitoba, Winnipeg, MB R3T 2N2, Canada*
[c] *Los Alamos National Laboratory, Los Alamos, NM 87545, USA*
[d] *The University of British Columbia, Vancouver, BC V6T 1Z1, Canada*
[e] *University of Winnipeg, Winnipeg, MB R3B 2E9, Canada*
[f] *Research Center for Nuclear Physics, Osaka University, Osaka 567-0047, Japan*
[g] *Nagoya University, Nagoya 464-8601, Japan*
[h] *KEK, Tsukuba 305-0801, Japan*
[i] *Simon Fraser University, Burnaby, BC V5A 1S6, Canada*
[j] *J-PARC, Tokai 319-1195, Japan*
[k] *Coburg University of Applied Science, 96450 Coburg, Germany*
[l] *University of Northern British Columbia, Prince George, BC V2N 4Z9, Canada*
[m] *SNOLAB, Sudbury, ON P3Y 1N2, Canada*
[n] *Technical University of Munich, 85748 Garching, Germany*
[o] *Indiana University, Bloomington, IN 47405, USA*
[p] *Institute of Modern Physics, Chinese Academy of Sciences, Lanzhou 730000, China*

arXiv:2208.05590v2 [nucl-ex] 7 Feb 2023

Abstract

Electroless nickel plating is an established industrial process that provides a robust and relatively low-cost coating suitable for transporting and storing ultracold neutrons (UCN). Using roughness measurements and UCN-storage experiments we characterized UCN guides made from polished aluminum or stainless-steel tubes plated by several vendors.

All electroless nickel platings were similarly suited for UCN storage with an average loss probability per wall bounce of $2.8 \cdot 10^{-4}$ to $4.1 \cdot 10^{-4}$ for energies between 90 neV and 190 neV, or a ratio of imaginary to real Fermi potential η of $1.7 \cdot 10^{-4}$ to $3.3 \cdot 10^{-4}$. Measurements at different elevations indicate that the energy dependence of UCN losses is well described by the imaginary Fermi potential. Some special considerations are required to avoid an increase in surface roughness during the plating process and hence a reduction in UCN transmission. Increased roughness had only a minor impact on storage properties.

Based on these findings we chose a vendor to plate the UCN-production vessel that will contain the superfluid-helium converter for the new TRIUMF UltraCold Advanced Neutron (TUCAN) source, achieving acceptable UCN-storage properties with $\eta = 3.5(5) \cdot 10^{-4}$.

Keywords: Ultracold neutrons, electroless nickel, storage lifetime, surface roughness

1. Introduction

Neutrons with energies below a few hundred nano-electronvolts, so-called ultracold neutrons (UCNs), are totally reflected by certain materials under all angles of incidence. Hence, they can be transported to experiments and stored in vessels for several minutes, making them perfectly suitable for precision measurements of the neutron's fundamental properties such as lifetime, beta-decay correlations, electric dipole moment, charge, and interaction with gravity. However, due to the low intensity of available UCN sources, these measurements often take years to gather competitive statistical precision.

To maximize the number of UCNs available to experiments, recent developments of UCN guides have focused on increasing transport efficiency by reducing diffuse neutron reflections, typically by exploiting the very small roughness that can be achieved on glass surfaces. Glass tubes can be coated with materials with high reflective Fermi potential like nickel, nickel alloys, or diamond-like carbon [1]. Or the properties of a glass surface can be replicated onto thin nickel-alloy sheets using the "Replika" technology [2]. The resulting guides are fragile, and seamlessly connecting them without gaps is challenging—gaps and slits often dominate losses in a UCN guide system. For

*Corresponding author
Email address: wschreyer@triumf.ca (W. Schreyer)

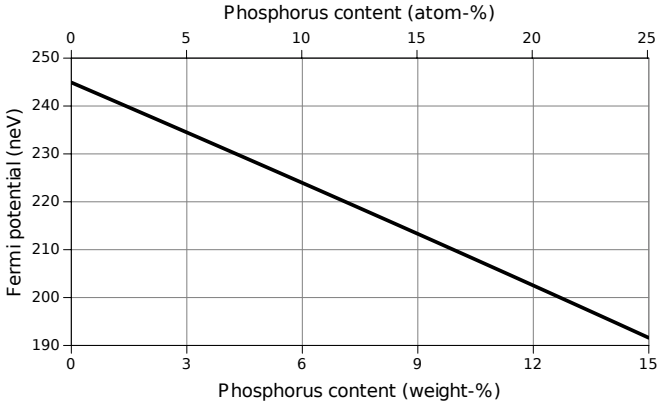


Figure 1: The Fermi potential of electroless nickel plating, calculated using neutron scattering lengths from [5] and densities from [6], drops with increasing phosphorus content.

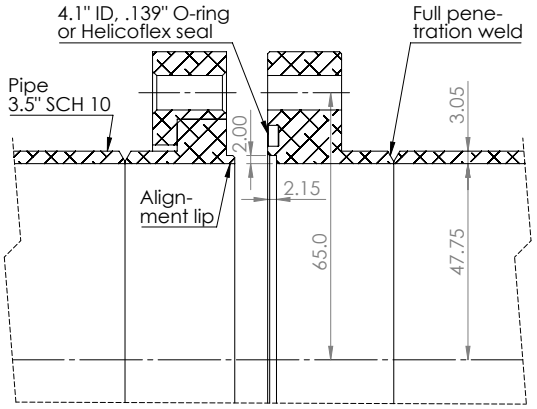


Figure 2: Design of UCN guides for the TUCAN source. All dimensions are given in millimeters.

these reasons, polished stainless-steel tubes that can be easily manufactured, cleaned, and connected are still widely in use.

The TRIUMF UltraCold Advanced Neutron (TUCAN) collaboration is building a new UCN source based on a superfluid-helium converter close to a spallation neutron source that is expected to surpass the intensity of existing sources by at least one order of magnitude [3]. To achieve this performance the converter needs to be contained in a large, thin-walled, superfluid-leak-tight, and radiation-tolerant vessel made from materials with low density and low neutron absorption; ideally an alloy of beryllium, magnesium, or aluminum. Beryllium is lightweight (1.8 g cm^{-3}), has a small neutron-absorption cross section (0.008 b), and has a high Fermi potential (251 neV), but is prohibitively expensive. Magnesium and aluminum have similar densities (1.7 g cm^{-3} to 2.7 g cm^{-3}) but higher neutron-absorption cross sections (0.06 b to 0.23 b) and low Fermi potentials (54 neV to 60 neV), requiring a robust, UCN-reflective coating. We did consider beryllium-aluminum [4] and magnesium-aluminum alloys [3], however these uncommon materials would have required specialized knowledge in machining, welding, and plating to fulfill the challenging requirements. We ultimately chose aluminum due to the large variety of available alloys and wealth of knowledge to complete the vessel within a reasonable time and budget.

Electroless nickel plating is a coating process that can deposit a nickel-phosphorus mixture onto a variety of substrates, including steel, aluminum, and copper, by immersing them into a bath. It is a well-studied and widely established industrial process used to increase hardness and wear resistance of surfaces and is offered by a large number of vendors at low cost. The phosphorus content can be varied from less than 4 weight% ("low-phosphorus") to 14 weight%, varying its metallurgical properties [6] and Fermi potential, see Fig. 1. The thickness of the coating can typically be tuned from 5 µm to 50 µm by simply adjusting the time for which the substrate is submersed in the bath. Hardness can be further increased with heat treatment after plating.

Electroless-nickel-plated guides and vessels have been successfully used in a prototype UCN source developed at the Research Center for Nuclear Physics, Osaka University [7, 8] and for an upgrade of the UCN source at Los Alamos National Laboratory [9]. Above a phosphorus content of 10 weight% ("high-phosphorus") the coating becomes non-magnetic, making it suitable for transporting polarized UCNs, as demonstrated by [10].

In an effort to find a vendor capable of plating the 2.67 m-long aluminum converter vessel for the new TUCAN source and UCN guides for a future TUCAN electric dipole moment (EDM) experiment, we used a variety of methods to characterize polished aluminum and stainless-steel substrates plated with electroless nickel by several vendors. We measured their roughness with a profilometer and we measured UCN storage lifetimes at the UCN sources at TRIUMF, Los Alamos National Laboratory, and J-PARC.

Based on the findings we selected a vendor to plate the converter vessel for the new TUCAN source and tested its UCN-storage properties at Los Alamos National Laboratory.

2. Sample preparation

In UCN-transport simulations of the new TUCAN source and EDM experiment we varied the guide diameters between 85 mm and 125 mm and achieved the best transport efficiency with guide diameters above 95 mm [11]. Hence, we chose a 3.5 in schedule 10 pipe standard with 4 in outer diameter and 0.12 in wall thickness, resulting in an inner diameter of 95.5 mm. For this pipe size we developed a new flange compatible with O-ring, *HELICOFLEX*, and diamond-shaped aluminum seals. An alignment lip ensures that guides are connected seamlessly and concentrically, see Fig. 2.

Irving Polishing & Manufacturing[1] polished these guides to a nominal roughness *Ra* (see section 3.1) of 51 nm to 76 nm (2 µin to 3 µin), with the exception of one guide, which was polished to 760 nm (30 µin).

[1] Irving Polishing & Manufacturing, Inc. 5704-46th Street, Kenosha, WI 53144, USA, `irvinginc.com`

We sent guides to three North American vendors for electroless nickel plating: *Chem Processing*[2] *Advanced Surface Technologies*[3], and *Dav-Tech Plating*[4]. *Chem Processing*, the same vendor used successfully for UCN guides by [9, 10], plated three 1 m-long guides, including the one with increased roughness. *Advanced Surface Technologies* plated three pairs of 0.5 m-long guides, including one pair with "black electroless nickel"—a coating that we hoped would provide similar UCN-storage properties but a lower reflectivity for thermal radiation [12]. *Dav-Tech Plating* plated one 1 m-long guide.

An additional 1 m-long stainless steel guide was manufactured in Japan, plated by *Asahi Precision*[5], and finally polished to a nominal roughness of 10 nm by *Ultra Finish Technology*[6].

All platings were specified to be 5 µm thick for aluminum substrates and 50 µm thick for stainless steel substrates, with a high phosphorus content of at least 10 weight%. The thicker plating on slightly magnetic stainless steel should reduce the UCN-depolarization probability [10].

Before any experiments with UCNs, we manually wiped the guides with a lukewarm 1 % solution of *Alconox* degreaser, de-ionized water, and isopropyl alcohol using *AlphaWipe* cleanroom cloths. To replace a guide in the experimental setup we vented the vacuum with nitrogen or argon gas, replaced the respective UCN guide, and then evacuated the system again to a pressure below $3 \cdot 10^{-5}$ mbar.

The converter vessel for the new TUCAN source consists of two aluminum hemispheres with an inner radius of 180 mm and a 2250 mm-long tube with an inner diameter of 148.2 mm, welded into one 2670 mm-long vessel with only one open end, see also Fig. 5. While the tube was again polished by *Irving Polishing & Manufacturing* to a nominal *Ra* of 51 nm (2 µin), the hemispheres were only electropolished, with the roughest areas receiving some additional manual polishing to bring the roughness below 1020 nm (40 µin).

The size of the parts to be plated are limited by the sizes of each vendor's plating baths, which were ∼1 m for *Chem Processing* and ∼0.5 m for *Advanced Surface Technologies*. *Dav-Tech* was the only vendor with baths large enough to plate the challenging geometry of the converter vessel, requiring some additional plumbing to maintain a steady flow of plating solution through the vessel. After plating, we cleaned the vessel by filling it with a 1 % solution of Alconox in de-ionized water and suspending an ultrasonic rod transducer into the solution for 20 min to 40 min. We repeated the ultrasonic cleaning with only de-ionized water, flushing and rinsing the vessel with de-ionized water before and after. Due to the size and shape of the vessel, wiping the inner surfaces with isopropyl alcohol was not possible. Unfortunately, the de-ionized water left more residue as expected and an improved cleaning method will be needed in the future.

[2]Chem Processing, Inc. 3910 Linden Oaks Drive, Rockford, IL 61109, USA, `chemprocessing.com`

[3]Advanced Surface Technologies, Inc. 6155 W 5th Ave, Arvada, CO 80002, USA, `astfinishing.com`

[4]Dav-Tech Plating, Inc. 40 Cedar Hill St, Marlborough, MA 01752, USA, `dav-techplatinginc.com`

[5]Asahi Precision Co., Ltd. 30-5 Kaide-Cho, Mukou, Kyoto 617-0004, Japan, `akg.jp/precision`

[6]Ultra Finish Technology Co., Ltd. 1-1-1 Heisei-Cho, Yokosuka, Kanagawa 238-0013, Japan, `uft.co.jp`

3. Measurement techniques

3.1. Profilometer and Ra roughness

We used a *Mitutoyo Surftest SJ-210* profilometer to measure the roughness of all guides at several positions along their length and circumference. The profilometer drags a diamond stylus across the surface to measure its roughness amplitude and can provide a set of different measures of surface roughness. We generally used the most common, standardized *Ra* measure to be able to compare to measurements done by the polishing companies. Localized scratches and imperfections in the plating can cause large outliers in roughness measurements, which we excluded from the data. We regularly checked the profilometer against a calibration sample with well-defined *Ra* and also confirmed that it can measure *Ra* roughnesses as small as 2 nm on a glass tube.

3.2. Storage of ultracold neutrons

To compare storage properties with varying experimental setups at several UCN sources we used a detailed analytical model taking into account the gravitational potential mgz along the elevation z and the neutron's beta-decay lifetime τ_β. The loss rate τ^{-1} for UCN with total energy $H = E + mgz$ can be calculated as

$$\tau^{-1}(H) = \frac{\sqrt{2H/m}}{4\gamma(H)} \int_a^b \frac{H - mgz}{H} \sum_i \frac{dA_i}{dz} \mu_i (H - mgz) dz + \tau_\beta^{-1}, \tag{1}$$

where a and b are the minimum and maximum elevation within the storage vessel, and

$$\gamma(H) = \int_a^b \frac{dV}{dz} \sqrt{\frac{H - mgz}{H}} dz \tag{2}$$

is the phase space available to UCN with total energy H. $\frac{dA_i}{dz}$ is the differential surface area covered by material i and $\frac{dV}{dz}$ the differential volume of the storage vessel at elevation z. Refer to [13, ch. 4.3] for a detailed explanation of this model.

The loss probability μ is calculated assuming an isotropic velocity distribution of UCN impinging on the surface with Fermi potential $U - iW$:

$$\mu(E) = 2 \int_0^{\pi/2} \left(1 - \left| \frac{\sqrt{E\cos^2\theta} - \sqrt{E\cos^2\theta - U + iW}}{\sqrt{E\cos^2\theta} + \sqrt{E\cos^2\theta - U + iW}} \right|^2 \right) \cdot \cos\theta \sin\theta d\theta. \tag{3}$$

Assuming a spectrum of UCNs $\frac{dN}{dH}$ initially filled into the storage vessel the number of remaining UCNs $N(t)$ at time t is then given by

$$N(t) = \int_{H_{\min}}^{H_{\max}} \frac{dN}{dH} \exp\left[-t \cdot \tau^{-1}(H)\right] dH. \tag{4}$$

Given a measurement of UCNs remaining in the vessel after different storage times we can fit the resulting curve with this model and determine the imaginary Fermi potential W. To compensate for detector noise and fluctuations in the source intensity, we determine the detector background rate and, where possible, estimate the UCN density delivered by the source using an independent normalization count N_n during each filling of the storage vessel. The detector count $N_d(t)$ is then corrected by subtracting the expected background counts N_b and dividing it by a normalization factor $N_n/\bar{N}_n$, where $\bar{N}_n$ is an average normalization count

$$N(t) = \frac{N_d(t) - N_b}{N_n}\bar{N}_n. \tag{5}$$

The energy spectrum provided by UCN sources is usually not very well known and is strongly shaped by guide geometry, guide materials, and energy-dependent detector efficiencies. Typically, it can only be indirectly inferred from simulations, which themselves have to make certain assumptions for these energy-dependent processes. Hence, we try to rely on simulations as little as possible and instead estimate parameterized spectra from simple principles while applying large uncertainties.

We include such systematic uncertainties by performing two fits for each model parameter, with its value set to the low end or the high end of its range while the other parameters are fixed to their central value. We then quote the mean W of the resulting set of results W_i and calculate its uncertainty as the square root of the quadratic sum of differences from the mean $\Delta W = \sqrt{\sum (W_i - W)^2 / 2}$. The factor $1/2$ in the sum accounts for the fact that we perform the fit twice for each parameter.

If the height of the storage vessel is small we can assume $\frac{dV}{dz} = V\delta(z - \bar{z})$ and $\frac{dA_i}{dz} = A_i\delta(z - \bar{z})$, simplifying the model for the loss rate to

$$\tau^{-1}(E) = \sqrt{\frac{2E}{m}} \sum_i \frac{A_i}{4V}\mu_i(E) + \tau_\beta^{-1} \tag{6}$$

where $E = H - mg\bar{z}$ is the kinetic energy at the center $\bar{z}$ of the storage vessel.

In simple storage experiments the energy-dependence of the loss rate is often ignored and instead an average storage lifetime $\bar{\tau}$ is determined by fitting a simple exponential model

$$N(t) = N_0 \exp\left(-t/\bar{\tau}\right). \tag{7}$$

We list the result of such a fit for each measurement as well.

We calculated the real Fermi potential U from neutron scattering lengths [5] and densities [6] for electroless nickel (EN) and stainless steel (SS), giving $U_{\mathrm{EN}} = 213(5)$ neV and $U_{\mathrm{SS}} = 183(5)$ neV, with uncertainties of 5 neV to account for any under- or over-estimations. This is also in good agreement with measurements by [9], which gave potentials for electroless nickel of 211(5) neV to 214(5) neV.

The imaginary Fermi potential correctly describes UCN losses if the loss cross section is indirectly proportional to the neutron velocity, which is the case for e.g. the nuclear-absorption cross section. From catalogued absorption cross sections [5] we expect imaginary Fermi potentials of about 0.023 neV for a high-phosphorus electroless nickel mixture and 0.019 neV for stainless steel. However, other loss processes, e.g. UCNs escaping through gaps, may be better described with an energy-independent loss probability $\mu(E) = \bar{\mu}$.

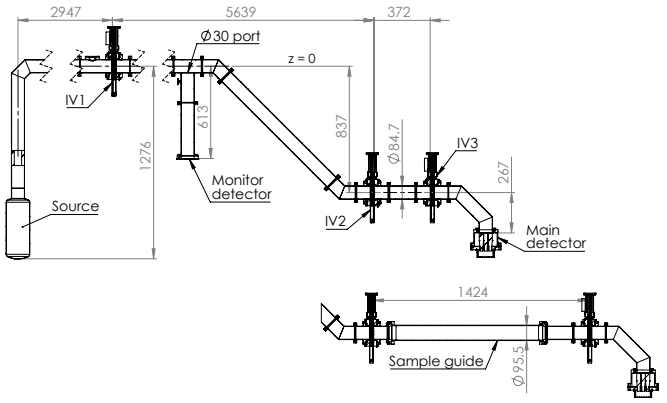


Figure 3: Side view of experimental setups to measure UCN storage lifetime using a prototype UCN source at TRIUMF. *Top*: baseline; *bottom*: with sample guide inserted. All dimensions are given in millimeters.

3.2.1. Storage of ultracold neutrons at TRIUMF

To measure UCN storage lifetimes in guides at TRIUMF we used a prototype UCN source shown in Fig. 3. UCNs are extracted vertically from a superfluid-helium converter and transported through stainless steel guides penetrating the radiation shielding, see also [8]. Where they exit the shielding, a monitor detector, a Dunia-10 ^{3}He proportional counter with an aluminum window, is attached to the guide through a 30 mm-diameter port. The main guide continues downwards 84 cm to the storage chamber.

Three valves—IV1, IV2, and IV3—are mounted in the beamline. To fill the storage chamber, we opened IV1 and IV2 and irradiated the neutron spallation target with protons to produce ultracold neutrons. After a filling period of 60 s we closed IV1 and IV2 and turned off the proton beam. UCNs are now stored between IV2 and IV3. After a storage period we opened IV3 and dumped the remaining UCNs into the main detector, a ^{6}Li-glass-based scintillation detector [14]. We varied the storage period from 2 s to 150 s to observe the exponential drop in the number of detected UCNs and determine the storage lifetime. The number of UCNs detected in the monitor detector during the storage and counting periods serves as normalization. During the storage periods we determined the average background rate in the main detector.

The valves are off-the-shelf *VAT 17.2 series* gate valves with a protective ring improving UCN transmission in the open state. We modified them with a shim plate to eliminate gaps between the vacuum-sealing blade and the attached guides, drastically improving their storage properties in the closed state [15].

Since we performed all measurements at the same elevation and the elevation difference within the sample guides is small we used the simplified equation (6) for the loss rate $\tau^{-1}(E)$.

Table 1: Assumed energy range $H_{\min}$ to $H_{\max}$ and spectral exponent α of UCNs filled into each UCN-storage setup with guide elevation $\bar{z}$, stainless steel surface area A_{SS}, electroless-nickel-plated surface area A_{EN}, and volume V; including setups with the new TUCAN source converter vessel (CV).

Setup	$H_{\min}$ (neV)	$H_{\max}$ (neV)	α	$\bar{z}$ (cm)	A_{SS} (cm^2)	A_{EN} (cm^2)	V (cm^3)
TRIUMF baseline	10(10)	92(10)	0.0(5)	-84	1109	0	2049
TRIUMF	10(10)	92(10)	0.0(5)	-84	1109	7476	9525
LANL1 high	10(10)	102(10)	0.95(50)	0	387	3073	7838
LANL1 low	10(10)	102(10)	0.95(50)	-84	387	3073	7838
LANL2 high	10(10)	102(10)	0.95(50)	-24	315	3226	8007
LANL2 low	10(10)	102(10)	0.95(50)	-108	315	3226	8007
LANL2 high (CV)	10(10)	102(10)	0.95(50)	-24	473	14956	67643
LANL2 low (CV)	10(10)	102(10)	0.95(50)	-108	473	14956	67643
J-PARC	64(10)	310(10)	0.75(75)	13	315	3226	8007

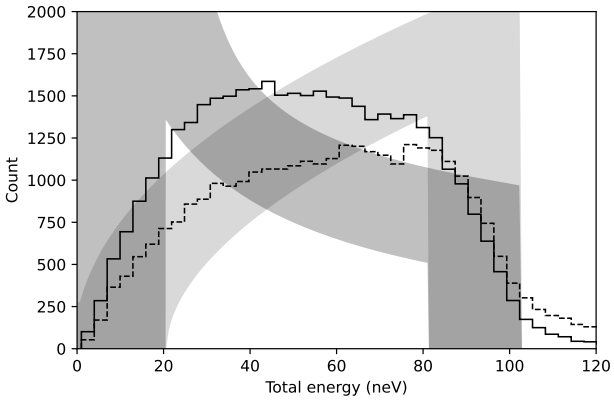


Figure 4: Simulated total-energy spectrum of UCN detected after a 0 s-long storage in the TRIUMF setup, assuming a $\sqrt{E}$ spectrum generated in the source and surfaces with imaginary Fermi potentials (solid line) and with energy-independent loss per bounce (dashed line). The shaded areas indicate the extremes of the assumed spectrum shape in the analytical model with α between -0.5 and 0.5 and $\Delta H = 10$ neV.

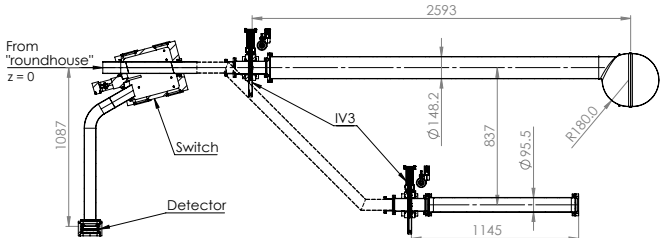


Figure 5: Side view of experimental setups to measure UCN storage lifetime at Los Alamos National Laboratory ("LANL1"), showing the TUCAN source converter vessel in the "high" position and a sample guide in the "low" position. A second set of measurements ("LANL2") was performed with a different switch that added an additional drop of 24 cm from the roundhouse. All dimensions are given in millimeters.

To estimate the energies of UCNs in the storage chamber, we assumed that the maximum energy of UCNs produced in the source is 213 neV, the Fermi potential of its electroless nickel plating. To exit the source the UCNs have to overcome an elevation difference from the bottom of the source vessel to the exit guide corresponding to a gravitational potential of 131 neV. The resulting spectrum of UCNs exiting the source is relatively narrow with energies between $H_{\min} = 0\,\text{neV} + \Delta H$ and $H_{\max} = 82\,\text{neV} + \Delta H$. Since energy cutoffs are typically not perfectly sharp, we added offsets $\Delta H = (10 \pm 10)$ neV with a large uncertainty.

Simulations of this source with PENTrack [16, 8] indicate that the stored spectrum is relatively flat, so we assumed an energy spectrum filled into the storage vessel of the form

$$\frac{dN}{dH} \propto (H - H_{\min})^{\alpha} \tag{8}$$

with an exponent $\alpha = 0.0 \pm 0.5$, again with a large uncertainty to account for any neglected effects that might modify the spectrum, see Fig. 4.

The valves and their adapters are bare stainless steel. We were able to measure its imaginary Fermi potential W_{SS} in a baseline experiment with only stainless steel surfaces, see Fig. 3. After adding an electroless-nickel-plated sample guide with two short adapters[7] we were able to subtract the losses on the stainless steel surfaces and calculate the imaginary Fermi potential W_{EN} of only the electroless nickel plating.

All relevant parameters—assumed energy spectra, elevations, surface areas, and volumes—are listed in table 1.

3.2.2. *Storage of ultracold neutrons at Los Alamos National Laboratory*

We also performed measurements with two sample guides and eventually the converter vessel for the new TUCAN source at the UCN source at Los Alamos National Laboratory (LANL). At the LANL source, UCN are produced in a solid-deuterium crystal and then vertically extracted. Previous studies of this source suggest that a connected storage volume will be filled with a velocity spectrum $dN/dv \sim v^{2.9}$ [17], corresponding to an energy spectrum[8] following equation (8) with $\alpha = 0.95 \pm 0.50$, where we again assumed a large uncertainty on the exponent. We performed our measurements at a beam port supplied through

[7] The adapters are polished aluminum plated by Chem Processing and 24 mm long.

[8] For a velocity spectrum $dN/dv \sim v^{\beta}$ the energy spectrum becomes $\frac{dN}{dE} = \frac{dN}{dv}\frac{dv}{dE} \sim v^{\beta} E^{-1/2} \sim E^{\beta/2-1/2}$.

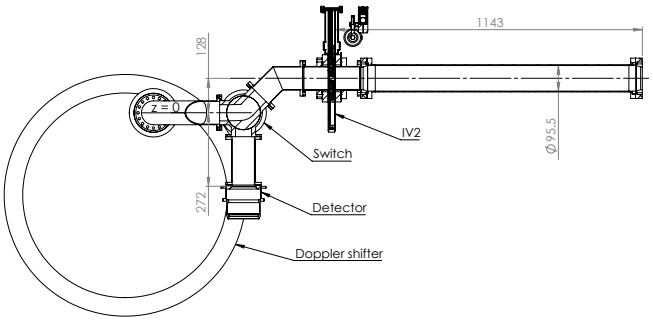


Figure 6: Side view of experimental setup to measure UCN storage lifetime at J-PARC. All dimensions are given in millimeters.

the "roundhouse", a large storage volume containing a UCN absorber at a height of 90 cm, limiting the UCN spectrum to energies between $H_{\min} = 0\,\text{neV} + \Delta H$ and $H_{\max} = 92\,\text{neV} + \Delta H$. Again, we added large uncertainties $\Delta H = (10 \pm 10)\,\text{neV}$, in part to take into account that UCNs with energies only slightly above the absorber threshold may take a long time to be absorbed.

The storage volume was filled for 200 s from the source, through a superconducting polarizer magnet, the roundhouse, a switch, and a storage valve, see Fig. 5. Then, we closed the storage valve and moved the switch to dump UCNs remaining in the guides into the ^{10}B-coated ZnS:Ag-scintillation detector [18, 19]; this count served as normalization. After a storage period of at least 20 s—the minimum time needed to completely empty the guides—we opened the valve again to count the UCNs remaining in the storage volume. During the following waiting period we measured the average background rate in the detector.

We performed the measurements at two elevations, a high position with switch and storage valve at the same level, and a low position with a vertical drop of 84 cm. For a second set of measurements including the converter vessel we used a different switch with an additional drop of 24 cm between roundhouse and switch.

To take into account the elevation changes and the larger elevation difference in the converter vessel we used the full equation (1) for the loss rate $\tau^{-1}(H)$. We assumed that the small portion of stainless steel surfaces have the same Fermi potential as was determined in the TRIUMF baseline measurement. All relevant parameters are listed in table 1.

3.3. Storage of ultracold neutrons at J-PARC

We performed another measurement at a UCN source at J-PARC, which uses a mirror mounted on a rotating arm to Doppler-shift a cold-neutron beam [20]. We extracted the resulting ultracold neutrons through an aluminum foil and filled them for 40 s through a switch with a 13 cm upward step and through a valve into the storage volume, see Fig. 6. Then we closed the valve to store UCNs while we moved the switch towards the detector and removed the UCNs remaining in the guides. After a storage period of 25 s to 125 s we opened the valve again and counted the remaining UCNs with a Dunia-10 ^{3}He proportional counter with aluminum window. During the waiting periods before and after counting we determined the average background rate in the detector.

Table 2: Measured roughnesses of UCN guides and converter vessel (CV) plated by *Chem Processing* (Chem Proc.), *Ultra Finish Technology* (UFT), *Advanced Surface Technologies* (AST), or *Dav-Tech Plating*.

#	Plating	Sub-strate	*Ra* roughness (nm) before plating	after plating
1	Chem Proc.	Al	54–62	87–197
2	Chem Proc.	Al	98–100	138–296
3	Chem Proc.	Al	744–752	850–976
4	UFT	SS	–	40–105
5	AST	Al	52–78	83–237
6	AST	SS	63–76	63–130
7	AST (black)	SS	62–76	105–1326
8	Dav-Tech	Al	50–75 (nom.)	254–737
CV	Dav-Tech	Al	38–64† (1040*)	374–626†

†Tube section only. *Max. roughness on hemispheres

Although we measured time-of-flight spectra of UCNs leaving the Doppler shifter, showing a flux strongly peaked at a velocity of 7.5 m s^{-1}, the spectrum filled into the storage volume is difficult to estimate. Hence, we assumed the spectrum follows equation (8) between $H_{\min} = 54\,\text{neV} + \Delta H$, the energy required to overcome the aluminum foil, and $H_{\max} = 300\,\text{neV} + \Delta H$ with potential offsets $\Delta H = (10 \pm 10)\,\text{neV}$, and with an exponent $\alpha = 0.75 \pm 0.75$ with a very large uncertainty. Since our model for the loss rate takes into account the quick loss of any UCNs above the Fermi potential of the storage volume the obtained results are not sensitive to the value of $H_{\max}$. Since we only performed measurements with the small sample guides, we used the simplified equation (6) to determine the imaginary Fermi potential. For the stainless steel surfaces in the storage volume we again assumed their Fermi potential is the same as measured in the TRIUMF baseline experiment. All relevant parameters are listed in table 1.

4. Results

4.1. Ra roughness

The electroless nickel plating provided by *Chem Processing* and *Advanced Surface Technologies* seems to typically increase the *Ra* roughness and its variability by up to 200 nm, independent of the substrate roughness, see table 2.

Although the roughness of the guide manufactured by *Ultra Finish Technology* was considerably lower than the others, we measured values well above the quoted roughness of 10 nm.

The "black" electroless nickel plating showed extreme variability in roughness.

The plating by *Dav-Tech* also had larger variability. Some test tube samples showed a continuous variation along the inner circumference with the minimal and maximal roughness 180° apart. This possibly stems from bubbles created during the plating process rising in the bath, adhering to the upper half of the

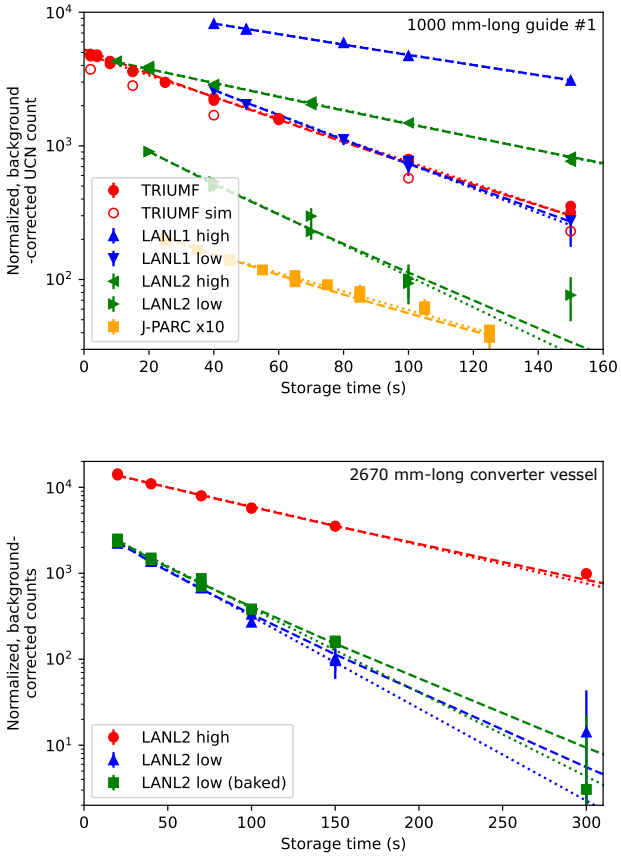


Figure 7: Number of UCNs counted after different storage times in reference guide #1 (top) and in the converter vessel (bottom) after background subtraction and normalization. Error bars are calculated from statistical uncertainties ($\Delta N = \sqrt{N}$) of main, monitor, and normalization counters. Dashed and dotted lines show fits with the detailed model (4) and with the average storage-lifetime model (7). The results from the low-intensity J-PARC source are averaged over up to 80 fillings to reduce statistical uncertainties and are shown scaled by a factor of 10. Simulations of the TRIUMF setup (empty circles) with $W_{\mathrm{EN}} = 0.04\,\mathrm{neV}$ and $W_{\mathrm{SS}} = 0.06\,\mathrm{neV}$ replicate the slope in the experimental data well.

inner surface, and intermittently disrupting the plating process. *Dav-Tech* was able to improve this variability by differently orienting some smaller samples in the plating bath.

Once the converter vessel was completed we were not able to measure roughness inside the hemispheres anymore, hence table 2 lists post-plating roughness only for the tube section.

4.2. Storage of ultracold neutrons

The UCN counts after different storage times in guide #1 and in the converter vessel are shown in Fig. 7. With the limited statistics and relatively short storage times neither the detailed model (4) nor the simple averaged storage-lifetime model (7) provided a consistently better fit.

The fit results for all measurements are shown in table 3. Despite the large systematic uncertainties in the energy spectra the estimated loss probabilities and imaginary Fermi potentials have uncertainties of less than 25 %. The statistical uncertainties are small in comparison, even when scaled with the poor χ^2 that is typical when fitting storage-lifetime measurements.

Table 3: List of storage setups (see table 1) with guide # (see table 2), their average storage lifetimes $\bar{\tau}$, energy-independent loss probabilities $\bar{\mu}$, and Fermi potentials $U - \mathrm{i}W$.

Setup	#	$\bar{\tau}$ (s)	$\bar{\mu}$ (10^{-4})	$U - iW$ (neV)
Baseline	–	31.4(8)	4.7(3)	183(5) – 0.055(10)i
TRIUMF	1	53.8(6)	2.8(2)	213(5) – 0.047(12)i
TRIUMF	2	53.1(6)	2.9(3)	213(5) – 0.048(13)i
TRIUMF	3	49.8(6)	3.2(3)	213(5) – 0.054(13)i
TRIUMF	4	41.8(6)	4.1(3)	213(5) – 0.071(16)i
TRIUMF	5	42.7(5)	4.0(3)	213(5) – 0.069(16)i
TRIUMF	6	47.2(6)	3.5(3)	213(5) – 0.059(14)i
TRIUMF	7	12.7(3)	18.1(12)	213(5) – 0.36(6)i
LANL1 high	1	112.5(25)	1.5(2)	213(5) – 0.047(11)i
LANL1 low	1	47.3(12)	3.2(2)	213(5) – 0.045(6)i
LANL1 high	8	127.4(46)	1.0(17)	213(5) – 0.037(9)i
LANL1 low	8	45.4(13)	3.4(2)	213(5) – 0.048(7)i
LANL2 high	1	85.7(29)	2.0(2)	213(5) – 0.046(8)i
LANL2 low	1	37.4(21)	3.9(4)	213(5) – 0.050(7)i
LANL2 high	CV	97.0(30)	3.4(2)	213(5) – 0.072(11)i
LANL2 low	CV	40.5(10)	6.2(5)	213(5) – 0.078(9)i
LANL2 low*	CV	44.4(15)	5.6(5)	213(5) – 0.070(8)i
J-PARC	1	62.6(18)	2.7(3)	213(5) – 0.049(16)i

*After 12 h baking at 100 °C

The imaginary Fermi potentials measured for guide #1 in different setups are compatible, providing confidence that our model is well suited to compare measurements across several UCN sources. Especially measurements at varying elevations provide compatible imaginary Fermi potentials, indicating that it correctly describes the energy dependence of UCN losses. In contrast, the estimated energy-independent loss probabilities show large variations between different energy ranges, indicating that losses are dominated by absorption or upscattering and not by UCN escaping through gaps.

The imaginary Fermi potential of the TUCAN source converter vessel turned out to be 50 % higher than the best guides. Baking the vessel at 100 °C for 12 h reduced the losses by 10 %. Earlier tests with a smaller electroless-nickel-plated storage vessel at TRIUMF already showed that baking at a higher temperature of 150 °C provides no further improvement.

We replicated the storage-lifetime measurements at TRIUMF with PENTrack simulations, see also [16, 8]. The imaginary Fermi potentials we used in the simulations to match the measured lifetimes fell well within the estimated uncertainties, see Fig. 7.

5. Conclusions

We successfully compared UCN-storage measurements of electroless-nickel-plated guides performed at several UCN sources. Guides plated by *Chem Processing* and *Dav-Tech* achieved the best storage properties, with imaginary Fermi potentials between 0.037 neV and 0.050 neV or ratios of imaginary to real

Fermi potential η between $1.7 \cdot 10^{-4}$ and $2.3 \cdot 10^{-4}$, a significant improvement over stainless steel with $\eta = 3.0 \cdot 10^{-4}$. [9] reported similar values between $1.1 \cdot 10^{-4}$ and $2.7 \cdot 10^{-4}$.

The "black" electroless nickel plating by *Advanced Surface Technologies* unfortunately was not suitable for UCN storage, causing high losses and a four times shorter storage lifetime. However, diamond-like carbon may be an alternative for a UCN-reflecting coating [21] that absorbs thermal radiation [22].

Ra roughnesses as large as 1000 nm seem to have little impact on the storage properties but larger roughness likely will negatively impact UCN transport. Although *Chem Processing* was able to achieve improved roughness compared to *Dav-Tech*, we had to choose *Dav-Tech* to plate the converter vessel for the new TUCAN source, as they were the only vendor capable of plating such a big vessel.

The UCN losses in the plated converter vessel were measured to be 50 % higher than in the best guides. However, simulations showed that that would have only a minor impact on the future TUCAN EDM experiment [11] since the losses in the source will be dominated by upscattering in the liquid helium converter. Hence, we consider the vessel acceptable for use in the new source. A closer inspection revealed that some residue was left after the de-ionized water rinse and we expect to be able to improve the storage properties with an improved cleaning procedure using an articulated arm to manually wipe the inner surface.

Acknowledgement

We would like to thank C. Marshall, S. Horn, and D. Rompen for engineering support; and B. Hitti and C. Dick for operational support of the helium liquefier at TRIUMF.

This research was supported by CFI project 36322, NSERC grant SAPPJ-201-00031, and JSPS KAKENHI grants 18H05230 and 20KK0069. The measurement at LANL was supported by Los Alamos National Laboratory LDRD Program (Project No. 20190041DR). The neutron experiment at the J-PARC Materials and Life Science Experimental Facility was performed under KEK S-type proposal 2019S03.

References

[1] G. Bison, B. Blau, M. Daum, L. Göltl, R. Henneck, K. Kirch, B. Lauss, D. Ries, P. Schmidt-Wellenburg, G. Zsigmond, Neutron optics of the PSI ultracold-neutron source: characterization and simulation, The European Physical Journal A 56 (2020). doi:10.1140/epja/s10050-020-00027-w.

[2] C. Plonka, P. Geltenbort, T. Soldner, H. Häse, Replika mirrors—nearly loss-free guides for ultracold neutrons—measurement technique and first preliminary results, Nucl. Instrum. Methods Phys. Res. A 578 (2007) 450–452. doi:10.1016/j.nima.2007.05.314.

[3] W. Schreyer, C. Davis, S. Kawasaki, T. Kikawa, C. Marshall, K. Mishima, T. Okamura, R. Picker, Optimizing neutron moderators for a spallation-driven ultracold-neutron source at TRIUMF, Nucl. Instrum. Methods Phys. Res. A 959 (2020) 163525. doi:10.1016/j.nima.2020.163525.

[4] AlBeMet Technical Fact Sheet, Materion Corporation, 2019. URL: https://materion.com/products/metal-matrix-composites/albemet.

[5] V. F. Sears, Neutron scattering lengths and cross sections, Neutron News 3 (1992) 26–37. doi:10.1080/10448639208218770.

[6] R. Parkinson, Properties and applications of electroless nickel, Technical Report, Nickel Development Institute, 1997. URL: https://nickelinstitute.org/media/1769/propertiesandapplicationsofelectrolessnickel_10081_.pdf.

[7] Y. Masuda, K. Hatanaka, S.-C. Jeong, S. Kawasaki, R. Matsumiya, K. Matsuta, M. Mihara, Y. Watanabe, Spallation Ultracold Neutron Source of Superfluid Helium below 1 K, Phys. Rev. Lett. 108 (2012) 134801. doi:10.1103/PhysRevLett.108.134801.

[8] S. Ahmed, et al. (TUCAN Collaboration), First ultracold neutrons produced at TRIUMF, Phys. Rev. C 99 (2019) 025503. doi:10.1103/PhysRevC.99.025503.

[9] R. Pattie, et al., Evaluation of commercial nickel–phosphorus coating for ultracold neutron guides using a pinhole bottling method, Nucl. Instrum. Methods Phys. Res. A 872 (2017) 64–73. doi:10.1016/j.nima.2017.07.051.

[10] Z. Tang, et al., Measurement of spin-flip probabilities for ultracold neutrons interacting with nickel phosphorus coated surfaces, Nucl. Instrum. Methods Phys. Res. A 827 (2016) 32–38. doi:10.1016/j.nima.2016.04.098.

[11] S. Sidhu, Improving the statistical sensitivity reach of the TUCAN neutron electric dipole moment experiment, Ph.D. thesis, Simon Fraser University, 2023, in preparation.

[12] R. J. C. Brown, P. J. Brewer, M. J. T. Milton, The physical and chemical properties of electroless nickel–phosphorus alloys and low reflectance nickel–phosphorus black surfaces, J. Mater. Chem. 12 (2002) 2749–2754. doi:10.1039/B204483H.

[13] R. Golub, D. J. Richardson, S. K. Lamoreaux, Ultra-cold neutrons, Adam Hilger, Bristol; Philadelphia, 1991.

[14] B. Jamieson, et al., Characterization of a scintillating lithium glass ultracold neutron detector, Eur. Phys. J. A 53 (2017) 3. doi:10.1140/epja/i2017-12195-7.

[15] D. Stang, Valve modifications and beam-envelope measurements towards the next generation ultracold neutron source at TRIUMF, Bachelor's thesis, Coburg University of Applied Sciences, 2020.

[16] W. Schreyer, T. Kikawa, M. Losekamm, S. Paul, R. Picker, PENTrack—a simulation tool for ultracold neutrons, protons, and electrons in complex electromagnetic fields and geometries, Nucl. Instrum. Methods Phys. Res. A 858 (2017) 123–129. doi:10.1016/j.nima.2017.03.036.

[17] T. M. Ito, et al., Performance of the upgraded ultracold neutron source at Los Alamos National Laboratory and its implication for a possible neutron electric dipole moment experiment, Phys. Rev. C 97 (2018) 012501. doi:10.1103/PhysRevC.97.012501.

[18] Z. Wang, C. Morris, Multi-layer boron thin-film detectors for neutrons, Nuclear Instruments and Methods in Physics Research Section A: Accelerators, Spectrometers, Detectors and Associated Equipment 652 (2011) 323–325. doi:10.1016/j.nima.2011.01.138, symposium on Radiation Measurements and Applications (SORMA) XII 2010.

[19] D. K. T. Wong, M. T. Hassan, J. F. Burdine, T. E. Chupp, S. M. Clayton, C. Cude-Woods, S. A. Currie, T. M. Ito, C. Y. Liu, M. Makela, C. L. Morris, C. M. O'Shaughnessy, A. Reid, N. Sachdeva, W. Uhrich, Characterization of the new Ultracold Neutron beamline at the LANL UCN facility, 2022. doi:10.48550/ARXIV.2209.00003.

[20] S. Imajo, K. Mishima, M. Kitaguchi, Y. Iwashita, N. L. Yamada, M. Hino, T. Oda, T. Ino, H. M. Shimizu, S. Yamashita, R. Katayama, Pulsed ultracold neutron production using a Doppler shifter at J-PARC, Progress of Theoretical and Experimental Physics 2016 (2016). doi:10.1093/ptep/ptv177, 013C02.

[21] F. Atchison, B. Blau, M. Daum, P. Fierlinger, P. Geltenbort, R. Henneck, S. Heule, M. Kasprzak, K. Kirch, K. Kohlik, M. Kuźniak, M. Meier, C.-F. Meyer, A. Pichlmaier, C. Plonka, P. Schmidt-Wellenburg, B. Schultrich, T. Stucky, V. Weihnacht, O. Zimmer, Storage of ultracold neutrons in a volume coated with diamondlike carbon, Phys. Rev. C 74 (2006) 055501. doi:10.1103/PhysRevC.74.055501.

[22] P. Hanzelka, T. Kralik, A. Maskova, V. Musilova, J. Vyskocil, Thermal radiative properties of a DLC coating, Cryogenics 48 (2008) 455–457. doi:10.1016/j.cryogenics.2008.03.021.